Conformational Changes of the Polysaccharide Cinerean in Different Solvents from Scattering Methods

M. Gawronski,[†,‡] H. Conrad,[†] T. Springer,*[,†] and K.-P. Stahmann[§]

Institut für Festkörperforschung, Forschungszentrum Jülich GmbH, D-52425 Jülich, Germany, and Institut für Biotechnologie, Forschungszentrum Jülich GmbH, D-52425 Jülich, Germany

Received March 20, 1996; Revised Manuscript Received September 9, 1996[⊗]

ABSTRACT: The conformation of cinerean, a microbial β-(1,3)(1,6)-D-glucan produced by the fungus *Botrytis cinerea*, was investigated in H_2O, NaOH, and DMSO by small-angle X-ray scattering (SAXS) and small-angle neutron scattering (SANS). The native cinerean is a wormlike chain with a large persistence length. By treatment with ultrasound rodlike fragments are formed. In aqueous solution cinerean has a multihelical conformation. In solutions with NaOH the cinerean multihelix disentangles into its single strands. These strands show the structure factor of a random coil. With scattering methods the transition between helix and coil was examined as a function of the pH value. SAXS measurements of the macroscopic scattering cross-section beyond the Guinier region yield directly the fractions α and $(1 - \alpha)$ of the single molecular strands in the "rod" or the "coil" state, respectively. The fraction α as a function of the pH value shows a narrow transition region at 0.15 N NaOH, which suggests a cooperative transition. The helix−coil transition is irreversible. A gel appears after neutralization of the solution. This gel is formed by multihelical rods acting as cross-links in a network of the molecular strands. In the organic solvent dimethyl sulfoxide (DMSO) a helix−coil transition was observed as well. For this measurement neutron scattering was used since the contrast between cinerean and DMSO for X-rays is very low.

Introduction

The microbial polysaccharide cinerean is a β-(1,3)(1,6)-D-glucan[1] produced as an extracellular energy storage by the fungus *Botrytis cinerea*.[2,3] It can be viewed as consisting of glucose and gentiobiose units forming a random copolymer.[4] From electron microscopy it is known that native cinerean is a wormlike chain with a large persistence length.[4] Treatment with ultrasound produces nearly rodlike fragments with an average length of about 70 nm.[4] In aqueous solution cinerean has a multihelical conformation accounting for the rigidity of the chain.[4,5]

We are interested in cinerean because of three aspects: the rheology, the importance as a model substance for very long and stiff molecules with their typical phase behavior[6] (as used for spinning and fiber production[7]), and the morphology. The rheology of cinerean is interesting because polysaccharides have technical importance[15] in enhanced oil recovery[16] and as gelation agents in the food industry. Already a few grams per liter of the native forms make aqueous solutions highly viscous. The aspect of cinerean as a model substance is treated elsewhere.[5] Rodlike molecules reveal a phase separation with a miscibility gap.[6] In an earlier paper we approximately calculated the phase diagram of sonicated cinerean.[4] We also examined the structure of the precipitated rod bundles in the miscibility gap.[5] The morphology of cinerean is of interest because certain D-glucans influence the immune system as unspecific modulators, which might be used to treat certain kinds of cancer.[8,9]

As will be shown in this paper, cinerean undergoes a helix−coil transition when dissolved in NaOH or DMSO. By breaking hydrogen bonds the multihelix with rodlike conformation disentangles into its single strands which form random coils. Several research groups have thoroughly examined the similar polysaccharides schizophyllan (produced by the fungus *Schizophyllum commune*) and scleroglucan (from *Sclerotium rolfsii*). In water these polysaccharides are triple helices.[10] In DMSO and aqueous NaOH they disentangle and become coils.[10] This helix−coil transition was studied with viscometry,[11] optical rotation,[11,12] and calorimetry.[12] Helix−coil transitions are important in biology, as they appear in proteins[13] and DNA.[14]

This paper deals with the morphology, and its goal is the examination of the conformational changes of cinerean depending on the pH value in aqueous NaOH solutions. Small-angle X-ray scattering (SAXS) allows us to determine independently the fractions of rods and coils from the scattering cross-section as a function of the scattering vector Q. In contrast to light scattering and viscometry, SAXS measurements for Q values beyond the Guinier regime are independent of the length distribution of the dissolved particles. In addition, it yields quantitatively the mass per unit length and the lateral radius of the rods, the pitch of the helix in the rodlike state, and the radius of gyration of the disentangled single chain, i.e. the spatial extension of the random coil. This is a new methodical aspect, which will be explained in the Results and Discussion. To our knowledge this is the first study which quantitatively examines such a helix−coil transition of cinerean in NaOH solutions with scattering methods.

Experimental Section

Cultivation of *B. cinerea* and Cinerean Production. The *B. cinerea* strain LU 1478 MaB was cultivated in a mineral salt medium, with D-glucose as the sole carbon source. The exact conditions for the cultivation and precipitation are described elsewhere.[3] The native cinerean was sonicated with a Branson B-15 P instrument (20 kHz, 150 W) in a pulsed mode with a duty cycle of 30% and an output control of 4 (ca. 60 W). An amount of 1.15 g of native cinerean was dissolved

‡ Present address: Institute for Chemical Research; Kyoto, Uji 611, Japan.
* Corresponding author.
† Institut für Festkörperforschung.
§ Institut für Biotechnologie.
⊗ Abstract published in *Advance ACS Abstracts,* October 15, 1996.

S0024-9297(96)00423-8 CCC: $12.00

in 115 mL of deionized water in a 250 mL beaker. During the sonication the sample was kept at about 8 °C. The sonication times were between 16 and 24 h. Scavengers for free radicals were not added. In order to remove metal fragments from the $^1/_2$ in. horn of the sonifier the sonicated sample was centrifuged at 42000*g* for 35 min. By adding 2-propanol the fragments were precipitated. After centrifugation at 4000*g*, the resulting pellet was dried in an argon flow until the weight remained unchanged. The length distribution of the fragments is rather narrow.[4]

Small-Angle X-ray Scattering (SAXS). The SAXS measurements were partly performed at the JUSIFA[17] small-angle scattering facility with a 100 kW rotating copper anode. Further measurements were carried out at an instrument at DESY/Hasylab in Hamburg with the DORIS storage ring as the X-ray source. The scattered intensity is measured with a two-dimensional position-sensitive detector. For absolute calibration a standard scatterer of amorphous carbon was used. The accuracy of the calibration is about 5%. The X-rays used had 8 keV from the rotating copper anode and 12 keV from the synchrotron.

Small-Angle Neutron Scattering (SANS). The SANS measurements were performed with the D 11 neutron small-angle camera[18] at the ILL in Grenoble and with the KWS 1 facility[19] at the research reactor DIDO in Jülich. The wavelengths of the neutrons were 0.6 and 0.7 nm. For calibration Lupolen and H_2O samples were used.

Chemicals. d-DMSO (99.8% d) was purchased from Merck.

Results and Discussion

Theoretical Background. The structure factor $S(\mathbf{Q})$ of a particle of volume V contains the information about the distribution of scattering centers in the particle, namely

$$S(\mathbf{Q}) = \left|\frac{1}{V}\int_V \mathrm{d}V \exp(-\mathrm{i}\mathbf{Q}\mathbf{r})\right|^2 \tag{1}$$

$\mathbf{Q}$ is the scattering vector; its absolute value is $Q = (4\pi/\lambda)\sin(\Theta) \approx 4\pi\Theta/\lambda$ with the scattering angle 2Θ and the wavelength λ of the incident radiation. $\mathbf{r}$ is the distance between scattering volume elements $\mathrm{d}V$. Obviously, $S(0) = 1$. The intensity $\Delta I(\mathbf{Q})$ scattered into a resolution element $\Delta\Omega$ of the detector is

$$\Delta I(\mathbf{Q}) = j_0 nfDT[K^2 S(\mathbf{Q})]\Delta\Omega \tag{2}$$

with $n = cN_A/M$ and $j_0 = I_0/f$. Here K is the "contrast" between the particle and the solvent, j_0 is the current density of the primary beam, f is the irradiated sample area, D is the sample thickness, T is the transmission of the sample, n is the number density of the particles, c is the concentration in g/cm^3 of the particles in the solution, N_A is Avogadro's number, M is the molecular mass of the particles, and I_0 is the primary intensity. For X-rays the contrast is $K^2 = (\mathrm{d}\sigma_{\mathrm{Th}}/\mathrm{d}\Omega)V^2(\Delta\rho_e)^2 = (\mathrm{d}\sigma_{\mathrm{Th}}/\mathrm{d}\Omega)M^2(\Delta z)^2$. Here $\mathrm{d}\sigma_{\mathrm{Th}}/\mathrm{d}\Omega$ is the differential scattering cross-section of the electron, $\Delta\rho_e$ is the average electron density difference between particle and solvent, V is the volume of the particle, M is its molecular mass, and Δz is the difference in mole of electrons per gram between particle and solvent. For neutrons the contrast is $K^2 = V^2(\Delta\rho_b)^2$ where $\Delta\rho_b$ is the scattering length density difference between particle and solvent. The scattering lengths can be found in tables.[22] For an isotropic system, an average over all particle orientations is to be taken and a small-angle experiment yields the macroscopic scattering cross-section

$$\mathrm{d}\Sigma(Q)/\mathrm{d}\Omega = \frac{\Delta I(Q)/\Delta\Omega}{I_0 DT} = nK^2 S(Q) \tag{3}$$

In the following we discuss the structure factors for a rigid rod and a random coil in different Q regimes. Because of the possible ternary structure of rods (if they consist of several molecules), the term "particles" instead of "molecules" is used below. For small Q one obtains, independent of the particle shape[20]

$$S(Q) = \text{const.} \times \exp(-Q^2 R_g^{\,2}/3) \tag{4}$$

R_g is the radius of gyration of the particle, which is the root mean square distance of the scattering centers from their center of gravity. With a Guinier plot ($\log(\mathrm{d}\Sigma/\mathrm{d}\Omega)$ vs Q^2), R_g and the molecular mass M can be determined.

Structure Factor of Rodlike Particles. For a cylinder with $x = L/(2R)$ (L = length, R = radius) the structure factor (after averaging over all orientations) is[23]

$$S(Q) = 4\int_0^{\pi/2} \frac{\sin^2(xQR\cos\gamma)}{x^2Q^2R^2\cos^2\gamma} \frac{J_1^{\,2}(QR\sin\gamma)}{Q^2R^2\sin^2\gamma} \sin\gamma\,\mathrm{d}\gamma \tag{5}$$

J_1 is the first-order Bessel function of the first kind, and $S(0) = 1$. For $1/L_{\mathrm{rod}} < Q < 1/R_c$ the structure factor can be simplified and is described by[20]

$$S(Q) = \frac{\pi}{L_{\mathrm{rod}}}\frac{1}{Q}\exp(-R_c^{\,2}Q^2/2) \tag{6}$$

R_c is the root mean square radius of the electron density distribution in a plane perpendicular to the rod axis (lateral radius of gyration). Assuming that the particles can be described as cylinders with a "sharp" surface filled homogeneously with electrons, we obtain $R = \sqrt{2}R_c$. In the case of a slightly bent rod ("wormlike chain"), eq 6 still holds if we replace L_{rod} by L_p, the persistence length, i.e. the distance between an arbitrary origin and a point along the chain at which the direction-cosine drops to an average value of 1/e.[20] (Rigid cylinder: $L_p = L_{rod}$.) Equation 6 with eq 3 leads to

$$\frac{\mathrm{d}\Sigma}{\mathrm{d}\Omega} = (\mathrm{d}\sigma_{\mathrm{Th}}/\mathrm{d}\Omega)\pi(\Delta z)^2 cN_A \frac{M_{\mathrm{rod}}}{L_{\mathrm{rod}}}\frac{1}{Q}\exp(-R_c^{\,2}Q^2/2) \tag{7}$$

Equation 7 is independent of the length distribution of the rods. Therefore, in the Q^{-1} regime, $\mathrm{d}\Sigma/\mathrm{d}\Omega$ only depends on the total length of all dissolved particles per unit volume. If the exponential function in eq 7 is close to unity, only the mass per length, M/L, of the rod is obtained, provided the macroscopic scattering cross-section is measured on an absolute scale. With light scattering the Q^{-1} regime cannot be reached for particles as small as those investigated here.

For larger scattering vectors ($Q \gg 1/R_c$) an asymptotic Q^{-4} regime prevails (Porod regime). For a particle with a smooth surface and a sharp step of $\Delta\rho_e$ or $\Delta\rho_b$ at the surface, the structure factor approaches

$$S(Q) = (2\pi/Q^4)\Psi/V^2 \tag{8}$$

where Ψ is the surface of the whole particle.[23] (For a monodisperse solution the structure factor oscillates around the Q^{-4} asymptote. (These oscillations cancel for a sufficiently broad distribution of R.) From the

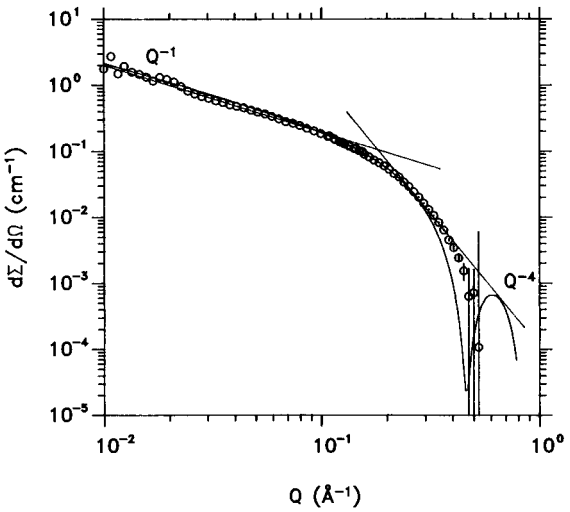

Figure 1. Macroscopic scattering cross-section dΣ/dΩ of fragmented cinerean in H_2O compared with the calculated structure factor. The typical Q^{-1} dependence for rodlike particles as well as the Porod Q^{-4} law are indicated by straight lines.

crossover region between the Q^{-1} and the Q^{-4} regimes both the mass per length M/L and the radius R of the rod can be calculated by plotting $\log(Q\, d\Sigma/d\Omega)$ vs Q^2 (eq 7). Thus one obtains independently the mass per length from two regimes of the scattering curve.

Structure Factor of Random Coils. In a random ("Gaussian") coil the monomers follow a random walk. For $Q < 1/l_s$ (l_s is the length of a statistical chain element) the corresponding structure factor is[20]

$$S(Q) = \frac{2}{Q^4 R_g^4}[\exp(-Q^2 R_g^2) - 1 + Q^2 R_g^2] \qquad (9)$$

For $R_g Q \gg 1$ an asymptotic Q^{-2} behavior is reached, namely, $S(Q) = 2/(Q^2 R_g^2)$, where $R_g^2 = N_s l_s^2/6 = l_{cont} l_s/6$ (N_s is the number of statistical chain elements and l_{cont} is the contour length of the chain, $l_{cont} = N_s l_s$). This yields the macroscopic scattering cross-section for large Q

$$\frac{d\Sigma}{d\Omega} = (d\sigma_{Th}/d\Omega)(\Delta z)^2\, cN_A \frac{12 M_{coil}}{l_{cont} l_s Q^2} \qquad (10)$$

where M_{coil} is the mass of a coil. In a Kratky plot (Q^2 dΣ/dΩ vs Q) (e.g. Figure 2A) a plateau is to be expected for the individual disentangled strands. Equation 10 shows that the cross-section is proportional to the mass per unit length, M_{coil}/l_{cont}. This is independent of the contour length distribution in analogy to the case for rigid rods (eq 7). In other words, for random coils in the Q^{-2} regime, dΣ/dΩ only depends on the total contour length of all dissolved coils per unit volume.

Cinerean and Schizophyllan in H_2O with X-rays. We studied fragmented cinerean and schizophyllan in aqueous solution with SAXS. Figure 1 shows the macroscopic scattering cross-section of fragmented cinerean in H_2O measured with X-rays as a function of the scattering vector Q compared with the calculated structure factor. The polydispersity of the rods (with the length distribution as determined with electron microscopy[4]) does not appreciably influence the result according to eq 5. With X-rays it was not possible to reach Q values smaller than 10^{-2} Å^{-1}. Thus the Guinier regime (eq 4) was not accessible. The Q^{-1} regime (eq 7), however, can clearly be seen. From this we conclude that cinerean has a nearly rodlike conformation.

Table 1. Mass per Unit Length, *M/L*, from Both the Q^{-1} Regime and a log(*IQ*) vs Q^2 Plot for Different Samples of Cinerean (NC, Native Cinerean; FC, Fragmented Cinerean) and Fragmented Schizophyllan (FS)[a]

		M/L Dalton nm^{-1}		
sample	*c* (mg/mL)	log(*I*) vs log(*Q*)	log(*IQ*) vs Q^2	av
NC03	10	2370 ± 470	2450 ± 390	2420 ± 300
FC04a	6	2350 ± 680	2510 ± 560	2440 ± 430
FC04b	12	2110 ± 470	2380 ± 410	2260 ± 310
FC04c	24	2610 ± 860	2870 ± 490	2800 ± 430
FC04d	50	2490 ± 480	2840 ± 440	2680 ± 330
FS02	25	1930 ± 360	2210 ± 350	2080 ± 250
FS03	25	1870 ± 340	2120 ± 330	2000 ± 240

[a] For a detailed discussion see text.

Table 2. Radius *R* of the Rigid Rods from a log(*IQ*) vs Q^2 Plot in Comparison to the Radius Calculated According to $R = ((M/L)/(\pi\rho))^{1/2}$ (Consistency Check)[a]

sample	*R* (10^{-1} nm) log(*IQ*) vs Q^2 (±0.2)	*R* (10^{-1} nm) from *M/L* (av)
NC03	9.1	9.4
FC04a	7.6	9.5
FC04b	7.8	9.1
FC04c	8.3	10.0
FC04d	8.0	9.9
FS02	7.6	8.7
FS03	7.8	8.5

[a] For details see text.

Table 1 shows results of the mass per unit length, M/L (eq 7), for several samples of cinerean (*N*ative *C*inerean and *F*ragmented *C*inerean) and schizophyllan (*F*ragmented *S*chizophyllan) using both the Q^{-1} regime and the crossover to the Q^{-4} regime. In Table 2 the results for the rod radii R are summarized. The samples FC04a-d are a concentration series from 6 to 50 mg/mL. Within the error limits no dependence of M/L or R on concentration is observed. This shows that interparticle interference and multiple scattering can be neglected. Within the errors the mass per length for all samples agrees rather well. Under the assumption that cinerean is a cylinder filled homogeneously with scattering medium we also calculated the radius from the mass per length with $R = \sqrt{(M/L)/(\pi\rho_m)}$ in order to check for consistency (Table 2); $\rho_m = 1.44$ g/cm^3 was used for the density.[9] The agreement between the two results is fair.

Other research groups have shown that schizophyllan has a triple-helical conformation in water ($M/L = 2170 \pm 50$ Dalton nm^{-1} and $D = 2R = 2.2 \pm 0.6$ nm).[10] This agrees fairly well with our SAXS results (Table 1). We conclude that cinerean has a triple-helical conformation as well.

Cinerean in NaOH Solution and in DMSO: Rod−Coil Transition. Figure 2 shows Kratky plots (Q^2 dΣ/dΩ vs Q) of the macroscopic scattering cross-section of cinerean (20 mg/mL) in 0.4 N NaOH solution and in H_2O (X-ray scattering, Figure 2A), compared with that of cinerean (20 mg/mL) in d-DMSO (neutron scattering, Figure 2B). The plateau between 0.1 Å^{-1} < Q < 0.3 Å^{-1} indicates that cinerean has changed its conformation from a rod to a Gaussian coil in NaOH and d-DMSO solutions. In this kind of plot the rodlike structure in H_2O yields a maximum. Its position is related to the effective radius of the rod by $Q_{max} = \sqrt{2}/R$.

Next we estimate the radius of gyration of the random coil formed by the cinerean molecule in NaOH. For

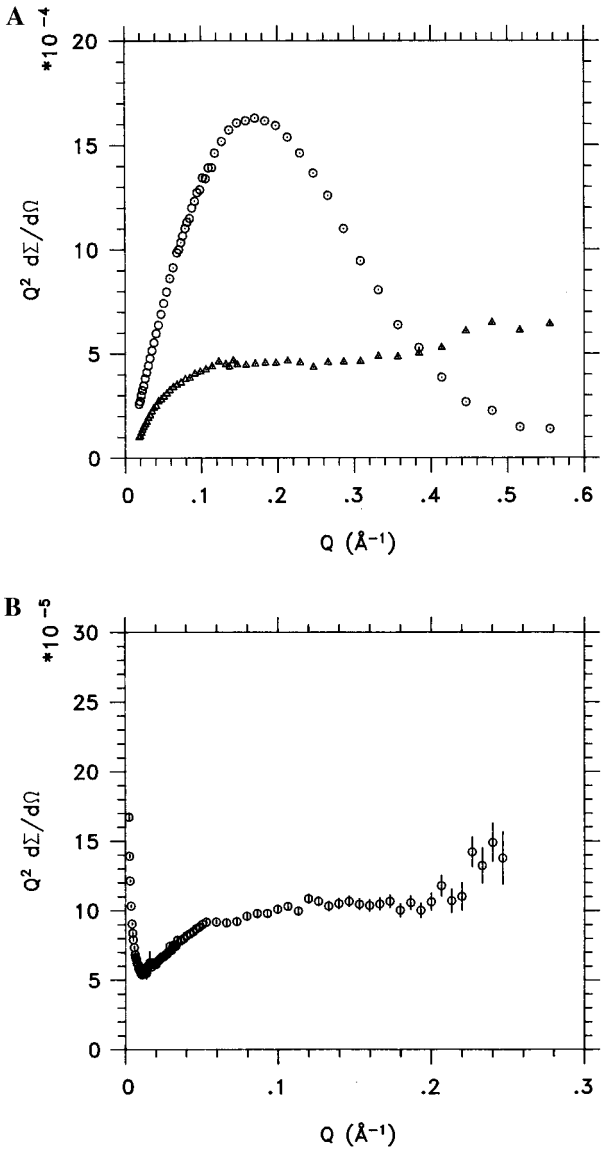

Figure 2. Kratky plots (Q^2 dΣ/dΩ vs Q) of cinerean (20 mg/mL): (A) in H_2O and in aqueous 0.4 N NaOH solution (SAXS); (B) in d-DMSO (SANS). The plateau is related to molecular coils, the peak to the (helical) rodlike particles.

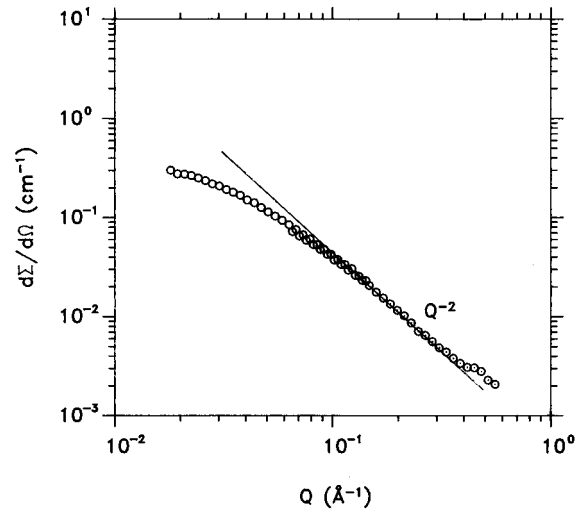

Figure 3. Macroscopic scattering cross-section dΣ/dΩ of cinerean in aqueous 0.4 N NaOH solution. From both the Q^{-2} dependence (indicating a random coil conformation) and the low-Q or Guinier regime the radius of gyration R_g of the coil can be consistently deduced (see text).

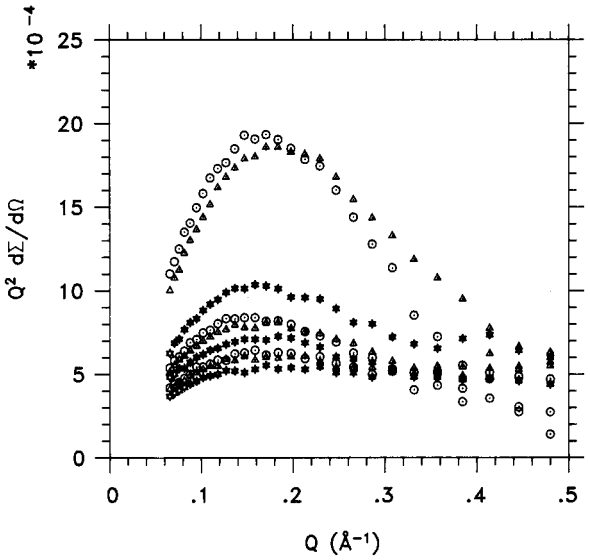

Figure 4. Kratky plots (Q^2 dΣ/dΩ vs Q) for fragmented cinerean (20 mg/mL) in aqueous NaOH solutions with normalities between 0 N (pure H_2O) and 0.22 N.

sufficiently small coils we obviously reach the Guinier-regime (Figure 3). For the measurement shown the results are $R_g = 4.3 \pm 0.2$ nm and M = 17000 ± 4000 Dalton. From the plateau in the Kratky-plot the radius of gyration was estimated as $R_g = \sqrt{2nK^2/((d\Sigma/d\Omega)Q^2)} \approx 4.0$ nm. This is consistent with the value from the Guinier region (Figure 3). This analysis cannot be carried out for the samples in d-DMSO because of agglomerations. Although the concentration was 20 mg/mL as in the case with hydrogenous solvents, the solution behavior is apparently different in deuterated solvents. Nevertheless, the data in the relevant Q regime still exhibit the typical plateau indicating the existence of random coils (Figure 2B).

As a microscopic mechanism for the disentanglement in H_2O we assume that the polysaccharide multihelix is stabilized by hydrogen bonds, by analogy with cellulose fibrils, i.e. intermolecular bonds between single strands and intramolecular bonds between one oxygen in the glycopyranose-ring and one hydrogen of the ring in the adjacent chain. The OH^- ions and the polar DMSO molecules replace these bonds so that the helix disentangles and the single strands become random coils.

Cinerean in Solutions for a Series of NaOH Concentrations. The helix−coil transition of fragmented cinerean (sonicated for 24 h) in a series of solutions with different NaOH concentrations was examined at room temperature with SAXS. All solutions contained the same amount of cinerean, i.e. 20 mg/mL. Due to the slow kinetics of the disentanglement process, the samples were prepared 1 week before the measurement in order to reach equilibrium. The result is shown in Figure 4. For cinerean in H_2O the curve has a maximum; the conformation is rodlike. With rising NaOH concentration this peak diminishes and for 0.22 N (normal) NaOH solution a plateau appears; the conformation of a Gaussian coil is reached. A thorough analysis shows that the maxima shift slightly to lower Q. This implies that the radius increases and that the helix swells before it disentangles into single strands. The change of R is of the order of a few 0.1 nm.

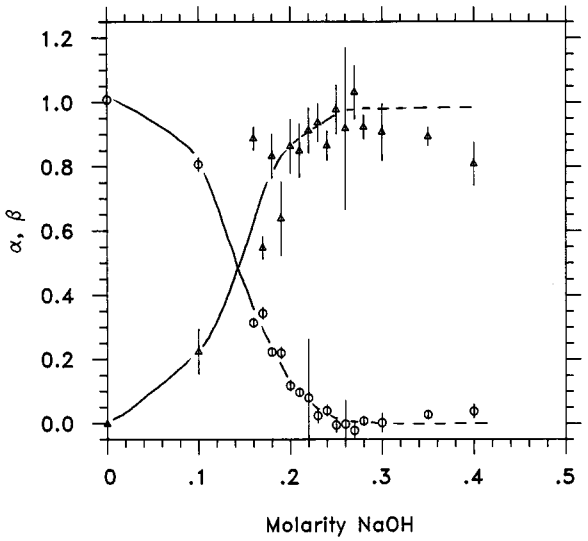

Figure 5. Fraction of rods (circles) and of coils (triangles) (from fitting eq 12) vs the molarity of the NaOH solutions. α and β are *independent* parameters. The lines are guides for the eye.

To quantify the relative amounts of rods (helices) and coils, we assume an incoherent superposition of the scattering cross-section for rods and coils; i.e. the scattering on the rods does not interfere with that on adjacent coils. This is a good approximation if the particles are either rods or coils or if interconnected rods and coils are sufficiently long. In the rods, h single strands are wound to form a multihelix; h is its multiplicity, e.g. $h = 3$ in our case. We define a factor $p \leq 1$ by which the helical rod is shorter than the strand contour length. Accordingly, the length of the helix (rod) is $L_{rod} = pl_{cont}$. The macroscopic scattering cross-section of the rods is then given by eq 7, and that of the coils by eq 10. This yields in the Q^{-1} and Q^{-2} regimes

$$\frac{d\Sigma}{d\Omega}|_{tot} = c(d\sigma_{Th}/d\Omega)(\Delta z)^2 N_A \times \frac{M_{coil}}{l_{cont}}\left\{\alpha\left[\pi h \frac{1}{p}\frac{1}{Q}\exp(-Q^2R^2/4)\right] + \beta\left[\frac{12}{l_s}\frac{1}{Q^2}\right]\right\} \quad (11)$$

The parameters α and β describe the weight fraction of dissolved particles in the "rod" and "coil" states, respectively. For $QR_g \gg 1$ this evidently follows from eqs 7 and 10. If our basic assumptions are correct, we should get $\alpha + \beta = 1$. For fitting we used the following parametrization:

$$\frac{d\Sigma}{d\Omega}\Big|_{tot} = \alpha A\frac{1}{Q}\exp(-BQ^2) + \beta\frac{C}{Q^2} \quad (12)$$

The constants A and B were found from the curve for $0.15\ Å^{-1} < Q < 0.3\ Å^{-1}$ in pure H_2O ($\alpha = 1, \beta = 0$) and the constant C by fitting in 0.4 N NaOH ($\alpha = 0, \beta = 1$) where the helices are disentangled completely. For all other curves eq 12 is fitted with these constants in order to determine the fraction of rods and coils, with α and β as independent parameters. Figure 5 shows these fractions. A sharp transition for about 0.15 N can be seen. Within the error limits the sum $\alpha + \beta$ is equal to 1; i.e. our assumption of independent superposition seems to be justified. Such a helix−coil transition is well-known for polypeptides.[13] By changing the solution parameters (temperature, pH, etc.), the hydrogen bonds

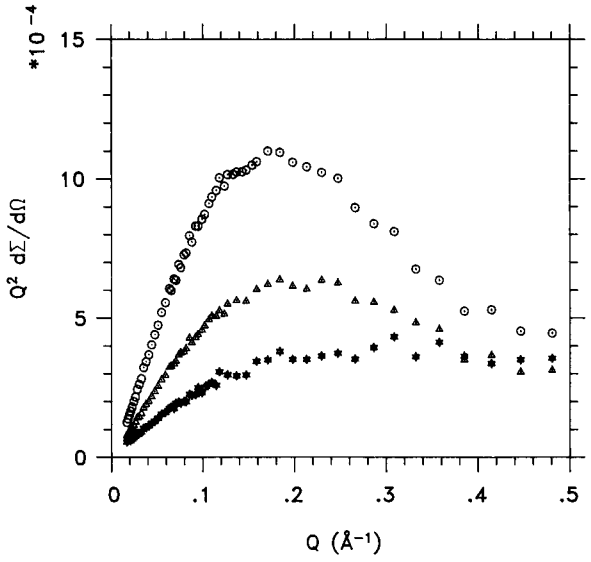

Figure 6. Kratky plots (Q^2 dΣ/dΩ vs Q) of cinerean (20 mg/mL) in 0.1 N NaOH solution dependent on the temperature: (circles) 25 °C; (triangles) 39.5 °C; (stars) 52 °C. At room temperature the conformation is entirely rodlike; at 52 °C it becomes a coil.

weaken and the rodlike polypeptide sections collapse and become coils. This transition is cooperative.

With an estimate for M_{coil}/l_{cont} and taking $h = 3$ for cinerean (by analogy with schizophyllan, Table 1), we can calculate the shortening factor p for the cinerean helix and the length of a statistical chain element l_s of the coil, using the constants A and C. $M_{coil}/l_{cont} \approx 315$ Dalton/nm was estimated from both the geometry of the glycopyranose rings and the knowledge that for cinerean the glucose−gentiobiose molar ratio is 1.38 ± 0.07.[4] Together with eq (11) this yields $p \approx 0.36$ for a triple helix. The statistical chain element of the coil has a length $l_s \approx 1.6$ nm, which corresponds to the length of about two glycopyranose rings. With this value for l_s and the radius of gyration $R_g \approx 4.0$ nm from above, we calculate the contour length as $l_{cont} \approx 60$ nm, corresponding to a length of the rod (helix) of $L_{rod} \approx 22$ nm. This is in good agreement with typical lengths of rods observed by electron microscopy.[4]

With rising temperature the transition point can be shifted to smaller NaOH concentrations. However, in pure H_2O a helix−coil transition was not observed, although the sample was stored at about 100 °C for 5 days. No release of reducing sugars or glucose was detectable by the Nelson−Somogyi method[24] or with hexokinase−glucose 6 phosphate dehydrogenase, respectively. From the detection limits of the methods we conclude that hydrolysis was less than 1% even after 5 days. Figure 6 shows the results for cinerean (20 mg/mL) in a 0.1 N NaOH solution. At room temperature the conformation is rodlike and at 52 °C it becomes a coil. The kinetics of the transition is quite slow: to reach equilibrium, the samples had to be stored for 5 days at the higher temperatures.

The helix−coil transition is not reversible. Figure 7 shows the results of related scattering experiments. First, a solution with 120 mg/mL cinerean in water was investigated. In the corresponding Kratky plot the peak indicates that cinerean is rodlike. Then 120 mg/mL cinerean in 1 N NaOH leads to a plateau and the particles have disentangled. Finally, this solution was neutralized with HCl. The resulting scattering curve exhibits a weak maximum (shifted to a smaller Q_{max}

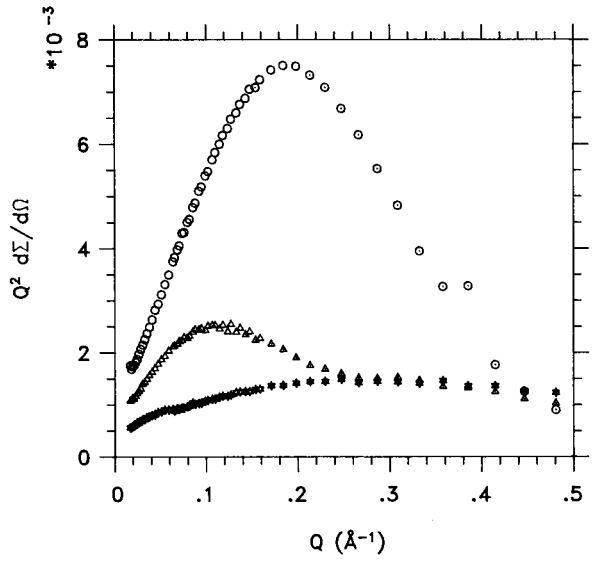

Figure 7. Kratky plots (Q^2 dΣ/dΩ vs Q) for a set of data showing the irreversibility of the disentanglement: (circles) cinerean (120 mg/mL) in H_2O (rodlike); (triangles) cinerean (120 mg/mL) in 1 N NaOH (completely disentangled, random coil); (stars) cinerean solution forming a gel after neutralization.

compared to that in water) and a plateau (overlapping with the plateau from the one in 1 N NaOH). Macroscopically, the neutralized sample became jelly-like. Consequently, we believe a network has developed, where single strands are cross-linked by incompletely reconstructed helical rods.

Conclusions

We investigated the solution behavior and structural properties of native and fragmented (sonicated) cinerean in NaOH and DMSO. For the first time, we observed a conformational transition of this polysaccharide in these solvents. We showed that small-angle X-ray and neutron scattering allows us to obtain conclusive structural information on these macromolecules in a single measurement. In H_2O fragmented cinerean has a rodlike, most probably triple-helical conformation. In NaOH and DMSO cinerean disentangles and the individual strands form Gaussian coils. In a series of solutions with different NaOH concentrations it was observed that the transition between helix and coil occurs in a relatively small pH range, where helices and coils are coexisting. With rising temperature the transition can be shifted to smaller NaOH concentrations. In H_2O at neutral pH cinerean is stable even up to 100 °C. The helix−coil transition is not reversible and, approaching neutralization, a gel is formed. Presumably, the disentangled strands establish cross-links by incompletely reconstructing the triple-helical conformation.

It is important to stress that in the Q^{-1} and Q^{-2} regimes exploited in the SAXS experiments the results are independent of the length distribution of the particles in the sonicated samples (in contrast to light scattering or viscometry). Obviously, this scattering method in the chosen regime is a powerful tool to consistently obtain the mass per unit length, the pitch of the helix in the rodlike state, the radius of gyration of the coil, i.e. its spatial extension, and independently, the fraction of molecules both as random coils and rigid rods in the transition state.

Acknowledgment. We thank T. Böddecker, U. Engelbrecht, G. Goerigk, H.-G. Haubold, P. Hiller, H. Jungbluth, P. Lindner, N. Monschau, M. Pionke, H. Sahm, G. Schmidt, D. Schneiders, and D. Schwahn for technical support and helpful discussions.

References and Notes

(1) Stone, B. A.; Clarke, A. E. *Chemistry and biology of (1,3)-beta-glucans*; La Trobe University Press; 1992.
(2) Montant, C.; Thomas, L. *Ann. Sci. Nat., Bot. Biol. Veg.* **1977**, *18*, 185.
(3) Stahmann, K.-P.; Pielken, P.; Schimz, K. L.; Sahm, H. *Appl. Environ. Microbiol.* **1992**, *58*, 3347.
(4) Stahmann, K.-P.; Monschau, N.; Sahm, H.; Koschel, A.; Gawronski, M.; Kopp, F.; Conrad, H.; Springer, T. *Carbohydr. Res.* **1995**, *266*, 115.
(5) Gawronski, M.; Aguirre, G.; Conrad, H.; Springer, T.; Stahmann K.-P. *Macromolecules* **1996**, *29*, 1516
(6) Flory, P. J. *Proc. R. Soc. London, A* **1956**, *234*, 73. Murthy, A. K.; Muthukumar, M. *Macromolecules* **1987**, *20*, 564. Miller, W. G.; Wu, C. C.; Wee, E. L.; Santee, G. L.; Rai, J. H.; Goebel, K. G. *Pure Appl. Chem.* **1974**, *38*, 37.
(7) Ballauff, M. *Angew. Chem.* **1989**, *3*, 261.
(8) Tabata, K. *Carbohydr. Res.* **1981**, *89*, 121.
(9) Franz, G., Ed. *Polysaccharide*; Springer: Berlin, 1991.
(10) Yanaki, T.; Kojima, T.; Norisuye, T. *Polym. J.* **1981**, *13*, 1135. Kashiwagi, Y.; Norisuye, T.; Fujita, H. *Macromolecules* **1981**, *14*, 1220. Norisuye, T.; Yanaki, T.; Fujita, H. *J. Polym. Sci., Polym. Phys. Ed.* **1980**, *18*, 547. Bluhm, T. L.; Deslandes, Y.; Marchessault, R. H.; Peres, S.; Rinaudo, M. *Carbohydr. Res.* **1982**, *100*, 117.
(11) Bo, S.; Milas, M.; Rinaudo, M. *Int. J. Biol. Macromol.* **1987**, *9*, 153.
(12) Kitamura, S.; Kuge, T. *Biopolymers* **1989**, *28*, 639.
(13) Zimm, B. H.; Bragg, J. K. *J. Chem. Phys.* **1959**, *31*, 526. Nagai, K. *J. Chem. Phys.* **1961**, *34*, 887. Cantor, C. R.; Schimmel, P. R. *Biophysical chemistry*; Freeman: New York, 1980.
(14) Takemoto, K. *Macromol. Chem. Suppl.* **1985**, *12*, 293.
(15) Sutherland, I. W. In *Extracellular Polysaccharides*; Rehm, H. J., Ed.; Biotechnology; Springer: Berlin, 1983.
(16) Holzwarth, G. *Dev. Ind. Microbiol.* **1985**, *26*, 271.
(17) Haubold, H. G.; Grünhagen, K.; Wagener, M.; Jungbluth, H.; Heer, H.; Pfeil, A.; Rongen, H.; Brandenberg, G.; Möller, R.; Matzerath, J.; Hiller, P.; Halling, H. *Rev. Sci. Instrum.* **1989**, *60*, 1943.
(18) Ibel, K. *J. Appl. Crystallogr.* **1976**, *9*, 296.
(19) Schwahn, D.; Meier, G.; Springer, T. *J. Appl. Crystallogr.* **1991**, *24*, 568.
(20) Glatter, O.; Kratky, O. *Small Angle X-Ray Scattering*; Academic: New York, 1982.
(21) Higgins, J. S.; Benoit, H. C. Polymers and Neutron Scattering; Clarendon Press: Oxford, U.K., 1994.
(22) *At. Nucl. Data Tables* **1991**, *49*, 65.
(23) Guinier, A.; Fournet, A. *Small Angle Scattering of X-Rays*; Wiley: New York, 1955.
(24) Nelson, N. *J. Biol. Chem.* **1944**, *153*, 375. Somogyi, M. *J. Biol. Chem.* **1952**, *195*, 19.

MA960423E